EIN2L, *EIL3*, and *EIL4* modulates drought resistance and growth by regulating stomatal movement in soybean

Meihan Ban[1†], Qiang Lv[1†], Jianfeng Liu[1†], Ian C. Dodd[2], Hongli He[1], Jiaqi Lv[1], Fanke Wang[1], Shuang Zhao[1], Xinyue Zhang[1], Hengshu Yu[1], Shuai Wang[1], Yang Zhao[1], Yunqing Cheng[1]*

[1]Jilin Provincial Key Laboratory of Plant Resource Science and Green Production, Jilin Normal University, Siping, Jilin Province 136000, China
[2]Lancaster Environment Centre, Lancaster University, Lancaster, Lancashire LA1 4YW, UK

*Correspondence: Yunqing Cheng
E-mail: chengyunqing1977@163.com
† Meihan Ban[†], Qiang Lv[†], Jianfeng Liu[†] **contributed equally to this work and share first authorship.**

Abstract

Soybean (*Glycine max*) is a globally important crop for oil, grain and feed; however, drought stress limits its yield and quality. Ethylene alters plant development, stress responses and yield, but the molecular mechanism(s) by which it regulates these processes have not been fully elucidated. Here we show the regulatory factors *EIN2L*, *EIL3*, and *EIL4* modulate stomatal movement and drought induced-ABA response. Plants with a triple *EIN2L*, *EIL3*, and *EIL4* CRISPR/Cas9 knockout showed attenuated darkness, ABA- and ethylene-mediated stomatal closure, with altered expression of genes related to ROS, NO and the anionic channels SLAHs. Furthermore, *EIN2L*, *EIL3*, and *EIL4* regulators positively regulate ethylene synthesis genes (*ACS* and *ACO*) during darkness and ABA synthesis (*NCED3)* and sensitivity (*PYL8*) genes following ABA treatment. Higher photosynthesis of well-watered plants and stomatal opening of the knockout lines, along with their diminished sensitivity to ABA, enhanced their water use thereby increasing their sensitivity to drought. Selecting for allelic variation in *EIN2L*, *EIL3*, and *EIL4* genes could better adapt soybean cultivars to the prevailing soil water availability, according to whether water conserving (WT alleles) or water-spending (knockout lines) traits enhance crop yields.

Keywords: soybean, stomatal movement, drought resistance, growth increment, ethylene, *EIN2*, *EILs*, signal integration

1 INTRODUCTION

Ethylene, a well-known senescence-related plant hormone, also regulates plant developmental process (Fatma et al., 2022; Khan, Ferrante, Khan, & Poor, 2023) and stomatal response to biotic or abiotic stresses in different species (Hasan, Liu, Yao, Liu, & Fang, 2024). Ethylene is synthesized from the amino acid methionine, with methionine adenosyl transferase catalyzing its transformation into S-adenosylmethionine (SAM). In turn, ACC synthase converts SAM to 1-aminocyclopropane-1-carboxylic acid (ACC), with ACC oxidase catalyzing the conversion of ACC to ethylene under aerobic conditions (Binder, 2020). Arabidopsis has five ethylene receptors (ETR1, ETR2, ERS1, ERS2 and EIN4) with their hydrophobic fragments embedded in the endoplasmic reticulum (ER) in the form of spiral, forming ethylene binding sites (Chang, Kwok, Bleecker, & Meyerowitz, 1993; Hua, Chang, Sun, & Meyerowitz, 1995). In the ethylene signal transduction pathway, the CTR1 protein (constitutive triple response), a serine/threonine protein kinase, is located downstream of the receptor ETR1, and negatively regulates the ethylene transduction pathway (Wang et al., 2006). The positive regulatory factor EIN2 is an endoplasmic reticulum integrin located downstream of ETR1/CTR1 complex that has a critical bidirectional function. When ethylene is absent or present in very low concentrations, binding of ETR1 with CTR1 to form the ETR1/CTR1 complex activates CTR1, phosphorylating the downstream EIN2, and preventing excision of the C end of EIN2, thus blocking signal transmission and inhibiting the physiological effect of ethylene. When various stresses increase plant ethylene concentrations to a certain

level, it binds to the receptor ETR1, thereby inhibiting the kinase activity of CTR1 and inactivating it. This decreases the phosphorylation level of EIN2, allowing its C end to be cut and enter the nucleus, inhibiting the downstream transcription factor EIN3 (F. Zhang et al., 2017). EIN3/EIL1 binds to the promoter of ethylene response genes such as ERFI (ethylene response factor) and EBF2 (EIN3-binding F-box protein 2) to induce gene transcription and expression of the gene, enabling ethylene-induced responses (Alonso et al., 2003; Chao et al., 1997; Solano, Stepanova, Chao, & Ecker, 1998). The F-box protein EBFI (EIN3-binding F-box protein I) and the ubiquitination of EBF2 also regulates the stability of EIN3 and EIL1 proteins, with EIN2 inhibiting the formation of EBF1/2 protein, thus leading to the accumulation of EIN3 protein (An et al., 2010; Potuschak et al., 2003). Unravelling these signal transduction pathways provides biotechnological opportunities to manipulate ethylene signaling *in planta*.

Light and CO_2 are the main abiotic factors regulating stomatal opening. Anion release from guard cells and subsequent depolarization of the plasma membrane are mediated by slow (S-type) and fast (R-type) anion channels (Schroeder & Keller, 1992). This anion efflux triggers membrane depolarization, which promotes K^+ efflux through outward-rectifying K^+ channels, ultimately leading to stomatal closure. In contrast, stomatal opening is primarily driven by the activation of H^+-ATPases in the plasma membrane (Kim, Böhmer, Hu, Nishimura, & Schroeder, 2010). These proton pumps extrude H^+ from guard cells, generating a hyperpolarized membrane potential that facilitates K^+ influx via inward-rectifying K^+ channels, accompanied by the uptake of anions such as Cl^- to maintain electroneutrality. Several studies have shown that exogenous ethylene decreases stomatal conductance according to the plant species and ethylene concentration applied (Ceusters & Van de Poel, 2018; Gunderson & Taylor, 1991; Hasan et al., 2024). In soybean (Glycine max), 21 μL L^{-1} ethylene approximately halved stomatal conductance (Ceusters & Van de Poel, 2018; Taylor & Gunderson, 1986), but the stomata of *Zea mays* did not respond, even when the ethylene concentration reached 10 000 μL L^{-1} (Pallaghy & Raschke, 1972). Ethylene-induced hydrogen peroxide (H_2O_2) synthesis mediating stomatal closure depends on activating the Gα subunit GPA1 (Ge et al., 2015). H_2O_2 in guard cells promotes the cleavage and nuclear localization of EIN2 via the MKK1/3-MPK3/6 signaling cascade (Zhang et al., 2021). Nitric oxide (NO) also plays a crucial signaling role in stomatal movement, mediating stomatal closure and thus regulating water balance and gas exchange in plants (Gayatri, Agurla, & Raghavendra, 2013; Hao et al., 2010). EIN3 can promote NO synthesis through a NR (Nitrate reductase)-dependent pathway (Shi, Chen, Peng, & She, 2017; Xin, 2010; Zhang et al., 2021). As a second messenger, NO always induces further downstream signaling by activating Ca^{2+} osmotic channels, leading to cytoplasmic Ca^{2+} increase and then activation of slowly activated anion channels (SLACs) and its homolog SLAHs. While these signaling pathways have primarily been elucidated in Arabidopsis, it is not clear whether these pathways regulate stomatal responses in other plant species such as soybean.

When plants experience drought stress, they quickly close their stomata to prevent excessive water loss with ABA playing a key role (Gupta, Rico-Medina, & Caño-Delgado, 2020). Drought stress triggers ABA synthesis primarily in mesophyll cells

(Kuromori et al., 2018), with subsequent accumulation in vascular bundle tissues and guard cells (Anfang & Shani., 2021). ABA accumulating in the guard cells regulates plasma membrane ion channels. Signaling molecules such as NO and reactive oxygen species (ROS) are components of ABA-mediated signaling cascades that control stomatal closure (Gong et al., 2021; Liu et al., 2023). Exogenous ABA (10 μM) treatment enhanced NO synthesis in guard cells, which plays a key role in ABA-induced stomatal closure (Gao et al., 2024; Majeed et al., 2020; Shen et al., 2021). Ethylene is hypothesized to participate in drought-induced stomatal closure along with ABA (Desikan et al., 2006) but can also inhibit ABA- and drought-induced stomatal closure in Arabidopsis (Tanaka et al., 2005, 2006; Watkins, Hechler, & Muday, 2014), and cotton (Kawakami, Oosterhuis, & Snider, 2010). Aged wheat leaves produce more ethylene and their stomata are less sensitive to soil drying and exogenous ABA application, which was restored by spraying leaves with the ethylene sensitivity inhibitor (1-MCP) or inoculating the soil with ACC-deaminase containing rhizobacteria, suggesting that both root-to-shoot ACC signaling and ethylene sensitivity are involved in stomatal regulation by dry soil (Chen, Dodd, Davies, & Wilkinson, 2013). Nevertheless, rewatering part of the soil substantially increased xylem ACC concentration and foliar ethylene evolution which was associated with transient stomatal closure (Perez-Perez et al., 2020), highlighting the variable impacts of ethylene on stomatal responses (Hasan et al., 2024). Investigating the stomatal responses of ethylene-insensitive plants to changes in darkness and soil moisture should further elucidate ethylene's involvement in stomatal regulation.

ABA-induced stomatal closure was significantly impaired in the Arabidopsis ACC synthase octahedral mutant, with accelerated stomatal response in the loss-of-function ethylene receptor double and single mutants *etr1-6 etr2-3* and *etr1-6*, while there was no significant change in stomatal response in the triple mutant *etr2-3 ein4-4 ers2-3*. Thus, ethylene biosynthesis and signaling components mediate the regulatory effect of ABA on stomatal conductance in *Arabidopsis thaliana* (Azoulay-Shemer et al., 2023), but different ethylene signaling components are involved. The pumpkin ethylene receptor CpETR2B enhances plant drought resistance by increasing accumulation of osmolytes and unsaturated fatty acids, with delayed stomatal closure of the *etr2b* mutant in response to soil drying (Iglesias-Moya et al., 2023). While germination and greening of the ethylene-insensitive Arabidopsis mutants *etr1* and *ein2-5* was more sensitive to osmotic stress (Wang et al., 2007), the physiological significance of higher foliar ABA concentrations in *ein2-5* to stomatal regulation is not clear. The diminished ability of *ein3-1* and *ein2-5* to accumulate osmolytes in response to osmotic stress compromised their water status and contributed to their lower survival rates (Cui et al., 2015), but stomatal responses were not investigated. Indeed, relatively few studies have investigated stomatal responses of ethylene-insensitive and WT plants to soil drying.

Previously, we demonstrated that a triple CRISPR/Cas9 knockout of the soybean (*Glycine max*) ethylene receptors *EIN2L*, *EIL3*, and *EIL4* enhanced growth and yield of field-grown plants (Cheng et al., 2023), which might be explained by altered photosynthetic responses to environmental stimuli. Thus, we evaluated leaf gas exchange and stomatal responses of wild-type and these gene-edited plants to

fluctuating light and soil moisture conditions. We hypothesized that ethylene insensitivity compromised stomatal responses to drying soil. Our investigation reveals that the *EIN2L*, *EIL3*, and *EIL4* constitute a core regulatory module that integrates upstream signals, including ethylene, drought-induced ABA and light-dark transition. In turn, this module alters the expression levels of ROS- and NO-generating genes, affecting anion channels genes that mediate stomatal movement, thereby regulating water use and photosynthetic efficiency. This module also regulates ABA synthesis and signaling and ethylene synthesis genes flexibly and quickly, allowing positive feedback responses to environmental stimuli.

2 MATERIALS AND METHODS

2.1 Plant materials and experimental design

Experiments at Jilin Normal University, Siping City, Jilin Province (longitude 124.345083, latitude 43.156557) used wild-type (WT) soybean (*Glycine max* cv. Williams 82) and a triple mutant (hereafter MU) obtained by editing the *EIN2L*, *EIL3*, and *EIL4* genes using CRISPR-Cas9 technology, which has early flowering and high yield phenotypes (Cheng et al., 2023). This knockout line, designated (Z4-1), was one of 3 lines generated that had similar agronomic responses. Plants were grown in pots (upper diameter, lower diameter and height were 20, 15 and 18 cm respectively) filled with about 6.0 kg of medium (3:1 mixture of local soil and vermiculite). Pots were uniformly spaced at 30 cm intervals. In all experiments, plants were watered every three days with 300 mL (grown in incubators) or 500 mL (outdoor plants) until the pot was dripping.

Plants were typically grown in LED light incubators (constant temperature 25℃) with 1.4 m^2 of growing space, set to a 12-hour photoperiod (08:00-20:00 h) and 60% relative humidity. To characterize plant morphology for 18 days after planting seed, the number of fully expanded trifoliate leaves, plant height, projected leaf area, and chlorophyll content of the youngest fully expanded leaf were measured (Supplementary Fig. 1). For subsequent experiments, 15 day-old plants at the V3-stage plants (third trifoliate fully expanded) were used for experiments as genotypic differences were minimal a this stage. To determine responses to a light-dark transition, after stomata were fully opened a dark treatment was imposed at 10:00 h (ZT2) followed by 0.75 h (ZT2.75) dark treatment and 0.75 h (ZT3.5) light recovery treatment. Thus samples were obtained at Light=ZT2, Dark=ZT2.75 and Re-lit=ZT3.5. Alternatively, leaves were sprayed with either 10 μM ABA, 400mg/L ethephon (ETH) or an aqueous ethanol solution (solvent control). Among them, ethephon treatment (ETH) was carried out in a separate incubator to avoid ethylene release affecting control plants. Treatments were applied at 10:00 until the solutions dripped from the leaves, and leaves sampled (for RT-qPCR analyses) after the solutions on the leaves had evaporated (about 0.5 h). In both types of experiment, lateral leaflets of the third trifoliate leaf numbering from the base of the plant were sampled for RT-qPCR analyses from three biological replicates (plants).

2.2 Stomatal aperture and density measurements

At the V3 stage, the third trifoliate leaf numbering from the base of the plant was selected. Three leaves from WT and MU plants were randomly selected. Leaves were excised with a sharp razor blade, the lower epidermal surface fixed with cellophane tape and the mesophyll removed with tweezers, and the lower epidermal surface retained. The slices were cut into small pieces and fixed on a microscope slide, with stomata imaged using a calibrated light microscope to determine stomatal aperture and density. The pore size was numerically calculated using image analysis software ZEN blue. The aperture value represents the average ratio of width to length of 20 pores in 5 fields of view. Stomatal density was determined as the number of stomata in 5 selected fields of view at a selected magnification of 40.

2.3 Total RNA extraction and RT-qPCR

Total RNA was extracted using the EasySpin RNA separation system (Aidlab Biotech, Beijing, China), and for qRT-PCR analysis, PrimeScript RT Reagent Kit (TaKaRa, Tokyo, China) was used according to the manufacturer's instructions. First strand cDNA was synthesized from 100 ng total RNA. The qRT-PCR analysis was performed using the SYBR premixed Ex Taq kit (TaKaRa) according to the manufacturer's protocol. The relative expression levels of selected genes were calculated using $2^{-\Delta\Delta Ct}$ (Schmittgen & Livak, 2008). Primers are provided in Table S1.

2.4 Immunohistochemical analysis

Young fully expanded leaves (the third leaf numbering from the base of the plant) were selected for immunohistochemistry, as previously described (Wei et al., 2021). Leaves were soaked with citrate buffer (pH = 6.0), microwaved and rinsed with distilled water after cooling. Then leaves were treated with PBS buffer twice, sealed with a drop of sealing solution, and incubated in a 37℃ incubator. Absorbent paper was used to dry the sealing liquid, with a single antibody (1:100) added to treatment and experimental groups and stored overnight in a 40℃ incubator. After the slides were taken out, treated with PBS and dried, the experimental group was added with horseradish peroxidase labeled secondary antibody (1:100), and the control group was added with distilled water and incubated at 37℃ for 30 min. After washing with PBS, add DAB (3, 3-N-Diaminobenzidine Tertrahydrochloride) to develop color. Finally, a light microscope (Axio Imager M2; Carl Zeiss, Jena, Germany) was used for imaging.

2.5 Water-loss and drought stress tolerance assays

At the V3 stage, young fully expanded lateral leaflets (the third leaf numbering from the base of the plant) were excised, placed in a petri dish containing desiccant at room temperature, and weighed every 30 min to determine their water-loss. Leaves were weighed until the weight remained unchanged, with water-loss rate calculated as: Water loss rate %=(W1-W2)/W1 (W1: Weight of isolated leaves before water loss W2: weight of isolated leaves after water loss * hours).

For drought stress tolerance assays, all plants were thoroughly watered at night until

water dripped from the pot. While the control group continued to be watered normally, water was withheld from the droughted treatment for 7 days, and then re-watered. Plants were randomly moved around in the incubator once a day to minimize the effects of uneven light distribution or air flow within the cabinet affecting water loss. On days 0, 7 and 14 after beginning the experiment, the above- and below-ground parts of WT and MU plants were photographed, scanned and determined by relevant indexes, respectively. Growth rate was calculated as shoot fresh weight after 14 days / shoot fresh weight after 0 days * 100 (%). Shoot water content was calculated as shoot fresh weight – shoot dry weight / fresh weight of above-ground part. Soil water content was calculated as fresh weight of soil - dry weight of soil/ fresh weight of soil. Various photosynthetic indexes were measured with a Li-6400(the light intensity was measured by the quantum sensor on the portable photosynthesis measurement system), leaf chlorophyll content and survival rate after 7 days of rehydration (survival rate = number of live plants / total number of plants *100%). If more than 70% of the plant leaves were desiccated, it was regarded as dead. Root morphological indices including root number and total length of roots were determined using a root scanner (EPSON 10000XL, China). Intact root samples were placed in the center of a 20 × 40 cm colorless transparent tray filled with deionized water, and roots were gently adjusted with forceps to avoid overlap before scanning. Root images were analyzed using the WinRhizo system (Regent Instruments, Canada) to quantify root parameters. The experiment was repeated 3 times

2.6 Light response curves and photosynthesis measurements

To compare daily variation in leaf gas exchange, seeds were planted in outdoor plastic pots in June 2023. When these plants entered the third phase (V3), photosynthetic parameters were measured in the 3rd leaf (numbering from the base of the plant) with a Portable Photosynthesis Measurement System (Li-6400, Li-Cor Inc., NE, USA) on a sunny day in the middle of July 2023. After entering the submenu of the automatic measurement program, the light response curve was measured from 08:00 h to 10:00 h (PPFD is about 800-1000 μmol·m^{-2}·s^{-1}) using the program "Light curve", which sequentially imposed PPFDs of 2000, 1500, 1000, 500, 200, 100, 50, and 0 μmol·m^{-2}·s^{-1}. Other parameters were adjusted to match ambient environmental conditions (CO_2 concentration of 400μmol·mol^{-1}, temperature of 26℃ and relative humidity of 45%), with net photosynthetic rate, stomatal conductance, intercellular CO_2 concentration and transpiration rate measured. Light saturation point and light saturation photosynthetic rate were calculated. Diurnal changes of net photosynthetic rate, stomatal conductance, intercellular CO_2 concentration and transpiration rate were measured every 2 hours from 06:00 to 18:00 h under ambient light conditions. (the light intensity was measured by the quantum sensor on the portable photosynthesis measurement system).

2.7 Detection and quantification of NO and ROS

Fluorescent probes DAF FM-DA (10 μM) and DCFH-DA (10 μM) were used to detect NO and ROS in soybean stomata (Gao et al., 2024; Zhang et al., 2021). Tear off the

lower epidermis and place it in MES buffer solution. Gently brush off the remaining mesophyll cells on it. After incubating under 100 μmol m^{-2} s^{-1} light for 3 h to open stomata, the strips were treated with probes in darkness at 25°C for 30 min, rinsed with MES buffer for 20 min, then exposed to ABA/ETH treatments for 30 min. Fluorescence was observed at 488 nm excitation/540 nm emission using a microscope, with intensity quantified via ImageJ.

To detect H_2O_2 and O_2^- in excised leaves using DAB and NBT (Xu et al., 2023), they were soaked in 50 μM DAB for 24 h or 50 mM NBT for 16 h, decolorized with 95% ethanol until white, and photographed.

2.8 Determination of ABA Content

High performance liquid chromatography (HPLC) was used to detect endogenous ABA content in leaves of two genotypes of plants, as previously described (Vine, Noiton, Plummer, Baleriola-Lucas, & Mullins, 1987) with some changes. Samples were ground in liquid nitrogen, extracted with acetonitrile and internal standard, centrifuged, and supernatants collected. Acetonitrile extraction was repeated twice, pooled, and dried under nitrogen. Chromatography used a Poroshell 120 SB-C18 column (2.1×150 mm, 2.7 μm) with mobile phases A (0.1% formic acid-methanol) and B (0.1% formic acid-water) at 0.3 mL/min. Gradient elution was performed at 30°C.

2.9 Promoter prediction

The potential binding sites of EIL3 transcription factor and promoter regions of *RBOHD/F, NIA1/2, SLAH1/3, ACS1/6, ACO1/4, ABF1/2/3* and other genes were predicted and analyzed. Promoter prediction using PlantPAN 4.0 (Chow et al., 2024) (https://plantpan.itps.ncku.edu.tw/plantpan4/index.html#hero), Data visualization uses TB tools (Chen et al., 2020; Chen et al., 2023).

2.10 Data analysis

Two-way ANOVA (main factors of genotype and treatment) were used in SPSS (Statistical Package for the Social Sciences) software, with a t-test evaluating statistically significant ($P < 0.05$) differences. GraphPad Prism 9.5.0 was used to draw the graphs, with experimental data expressed as mean values with standard deviations.

3 RESULTS

3.1 *EIN2L* mediates stomatal movement

Nyctinastic movement (nocturnal downward bending of leaves of well-watered plants) of WT plants occurred with 0.5 h of dark treatment, while leaves of MU plants remained relatively upright until 0.75 h of dark treatment (Fig. 1a). Projected leaf area of WT and MU plants was similar in the light, but WT plants had 21% and 11% lower leaf area than MU plants after 0.5 h and 0.75 h of dark treatment respectively (Fig. 1b). While stomatal density was similar in MU and WT plants (Fig. 1c), stomata of WT plants almost completely closed in the dark, but stomata of MU plants remained partially open

in the dark (Supplementary Fig. 2a-b). Stomatal conductance of MU plants was significantly higher than WT plants throughout light and dark transitions (Fig. 1d). Thus *EIN2L*, *EIL3* and *EIL4* seem involved in regulating leaf and stomatal movements.

Dark conditions significantly upregulated gene expression levels of *EIN2L*, *EIL3* and *EIL4* by 10-, 8- and 3-fold compared to light conditions (Fig. 1e). Restoring light after 0.75 hours of darkness significantly decreased expression levels of these genes. Of the 3 genes, *EIN2L* had the strongest response to light and dark transitions. To verify *EIN2L*, *EIL3* and *EIL4* involvement in stomatal movements, immunohistochemistry explored expression of *EIN2L*, *EIL3* and *EIL4* proteins in stomata of WT plants. Compared with the negative control, the *EIL3* and *EIL4* proteins did not seem to be expressed in guard cells (Fig. 1f). Since the *EIN2L* protein is expressed in guard cells, it seems to play an important role in mediating stomatal movement.

3.2 Impaired stomatal closure reduced drought resistance of the mutant

Under constant temperature and light conditions, detached WT leaves (Fig. 2a) lost water more slowly than detached MU leaves, but both lost the same amount of water after 2 hours (Fig. 2b). ABA treatment decreased the rate of water loss of WT leaves, but had no significant effect on MU leaves. Well-watered MU plants grew better (Fig. 2c-d), such that shoot growth rate was 2.5 times that of WT (Fig. 2e), while root number and length increased by 70% and 85%. This growth advantage was reversed following 7 days of drought and 7 days of rehydration, with survival rate of MU plants (50%) significantly lower than WT plants (80%) (Fig. 2f), and shoot growth rate 40% lower than WT plants (Fig. 2e). Shoot water content of WT plants was more stable during drought and 15%-30% higher than MU plants (Fig. 2g), and the soil moisture content was the same (Fig. 2h). Chlorophyll content of MU plants did not differ after the drought treatment, but was 30% lower than WT plants after rehydration (Supplementary Fig. 3a). Stomatal conductance (Fig. 2i), photosynthetic rate (Supplementary Fig. 3b) and transpiration rate (Supplementary Fig. 3c) of well-watered or droughted WT plants were significantly lower than MU plants, but these effects were reversed after rehydration. Intercellular CO_2 concentration of well-watered or droughted WT plants was higher than MU plants (Supplementary Fig. 3d), with an opposite response following rehydration. Seven days of drought reduced MU plant root growth versus controls. Root regeneration ability of MU plants after rehydration was less than in WT plants, with half as many roots and 24% less root length than WT plants (Fig. 2j-k). While well-watered MU plants grew better than WT plants, their higher stomatal conductance and reduced stomatal sensitivity to ABA made than more drought-sensitive than WT plants, as *EIN2L*, *EIL3* and *EIL4* genes are involved in drought-induced stomatal closure.

For outdoor-grown plants, stomatal conductance of MU and WT plants increased with light intensity until 1500 $\mu mol \cdot m^{-2} \cdot s^{-1}$, then declined as light intensity increased further (Supplementary Fig. 3e). At the same light intensity, stomatal conductance and transpiration rate (Supplementary Fig. 3f) of MU plants were 7% and 20% higher than

WT plants. As light intensity increased, intercellular CO_2 concentration (Ci) decreased similarly in MU and WT plants, although Ci of MU plants was lower than WT plants (Supplementary Fig. 3g). Curve fitting shows that photosynthetic light compensation point was similar in MU and WT plants, but MU plants had higher light saturation point (1500 $\mu mol \cdot m^{-2} \cdot s^{-1}$ *versus* 1300 $\mu mol \cdot m^{-2} \cdot s^{-1}$) and maximum net photosynthetic rate (22 $\mu mol\ CO_2 \cdot m^{-2} \cdot s^{-1}$ *versus* 17 $\mu mol\ CO_2 \cdot m^{-2} \cdot s^{-1}$) than WT plants (Supplementary Fig. 3h). Whereas light intensities exceeding 1500 $\mu mol \cdot m^{-2} \cdot s^{-1}$ decreased photosynthesis of WT plants, MU plants maintained photosynthesis.

Diurnal measurements of leaf gas exchange in outdoor-grown plants indicated higher stomatal conductance (Supplementary Fig. 3i) and transpiration rate (Supplementary Fig. 3j) of MU plants than WT plants, while Ci showed the opposite pattern (Supplementary Fig. 3k). Stomatal conductance of both genotypes increased from 06:00 h and peaked at 10:00h, then declined over the rest of the day. Net photosynthetic rate of MU plants peaked earlier (at 10:00 h) than WT plants that peaked at 12:00 h (Supplementary Fig. 3l). Mutant plants had higher maximum photosynthetic rate (24 $\mu mol\ CO_2\ m^{-2} \cdot s^{-1}$) than WT plants (20 $\mu mol\ CO_2\ m^{-2} \cdot s^{-1}$). Higher stomatal conductance of MU plants in (natural and controlled) light and darkness diminished their ability to regulate water loss as the soil dried.

3.3 Darkness promotes the expression level of NO and ROS synthesis related genes and anion channel SLAHs.

Transcription levels of genes encoding respiratory burst oxidase homologous proteins (RBOHs) were measured in light and dark conditions. Darkness increased expression of both *RBOHF* and *RBOHD* genes in WT plants by more than 10 times (Fig. 3a), and more than 20 times (Fig. 3b) respectively compared to Light and Re-lit conditions. These changes were attenuated in MU plants such that *RBOHF* expression only increased 3-fold times, and *RBOHD* expression only doubled. Gene expression levels were similar between genotypes in Light and Re-lit conditions. Expression of the *NIA1* gene (encoding nitrate reductase and producing NO *in vivo*) showed similar patterns, increasing more than 10-fold and 4-fold in WT and MU plants respectively in the Dark conditions, and with no genotypic differences in Light and Re-lit conditions (Fig. 3c). In contrast, expression of the *NIA2* gene was always higher in WT plants than MU plants irrespective of Light conditions (Fig. 3d). Re-lighting significantly down-regulated both NIA genes in WT plants, but expression of the *NIA2* gene remained higher in MU than WT plants.

Genes encoding the anion channels *SLAH1* and *SLAH3* showed similar patterns, with darkness upregulating their expression in WT plants, but with an attenuated response in MU plants. While *SLAH1* gene expression was more than 2-fold higher in WT plants than MU plants under Light conditions, Re-lit conditions reversed this response such that *SLAH1* gene expression was 69% higher in MU plants than WT plants (Fig. 3e). However, *SLAH3* gene expression was similar between genotypes when plants were lit (Fig. 3f). Thus, impaired dark-induced stomatal closure of MU plants may be due to perturbed signaling pathways of the slow anion channels *SLAH1* and *SLAH3*.

Expression of ethylene synthesis genes (ACC synthase 1 and 4, ACC oxidase 1 and 4) increased in both WT and MU plants during the Dark conditions, but more so in WT plants. Re-lighting resulted in similar gene expression of both genotypes (Fig. 3g-j). Taken together, dark-induced stimulation of ethylene synthesis induces stomatal closure by increasing NO and ROS accumulation, thereby mediating the expression of SLAHs, with *EIN2L* a key receptor.

3.4 *EIN2L* gene mediates ethylene signaling and promotes stomatal closure

Without ethephon treatment, stomatal aperture did not differ between genotypes (Supplementary Fig. 4a). Applying ethephon induced stomatal closure of both genotypes, but more so in WT plants such that their aperture was 28% higher than MU plants (Supplementary Fig. 4b). After ethephon treatment, stomatal conductance (Fig. 4a), net photosynthetic rate (Supplementary Fig. 4c) and transpiration rate (Supplementary Fig. 4d) of WT plants decreased by 70-80%respectively, and the intercellular CO_2 concentration increased by 71% (Supplementary Fig. 4e). In contrast, MU plants showed only 50% changes in these gas exchange variables. Photosynthetic parameters of MU plants were always higher than in WT plants, but intercellular CO_2 concentration had the opposite effect. Ethephon caused leaves of WT plants to senesce and abscise over time (Supplementary Fig. 4f), with chlorophyll content decreasing (Supplementary Fig. 4g), but MU plants were unaffected. Ethephon application confirmed that MU plants were ethylene-insensitive.

To further discern the mechanism of *EIN2L* mediated stomatal closure, transcription levels of genes *RBOHD*, *RBOHF*, *NIA1* and *NIA2* were measured before and after ethephon treatment (Fig. 4b-e, Supplementary Fig. 6a-d). Ethephon application significantly increased expression levels of these 4 genes in WT plants, more than 30 times for *RBOHD*, more than 6 times for *NIA1* and more than 5 times for *RBOHF* and *NIA2*. Transcription levels of these 4 genes in MU plants were significantly lower than WT plants (except for *RBOHD* without ethephon treatment), but still increased with ethephon treatment. Faced with this situation, NO and ROS levels in WT and MU plant stomata were measured. The result shows that ethephon treatment significantly increased guard cell NO levels in WT plants, but these remained low in MU plants (Fig. 4f-g), indicating impaired ethylene-induced NO accumulation. Similarly, ethephon triggered marked ROS accumulation in WT guard cells and leaves (including H_2O_2 and O_2^-), whereas MU plants showed minimal ROS response (Fig. 4h-I, Supplementary Fig. 4h-i). Thus ethylene regulates stomatal movement by inducing ROS in WT plants, but this pathway is disrupted in MU plants.

Meanwhile, expression levels of the genes *SLAH1* and *SLAH3* were higher in WT than MU plants independent of ethephon treatment (Fig. 4j-k, Supplementary Fig. 6e-f). While ethephon significantly increased the expression of both genes, WT plants showed a greater response. Similar gene expression responses to both darkness and ethylene suggests that dark-induced stomatal closure may be closely related to ethylene.

Before ethephon treatment, WT plants had higher expression levels of the ethylene

response factor 197 (but not *ERF*144) and *EBF* genes. Ethephon treatment significantly increased expression of all 3 genes in WT plants (Supplementary Fig. 4j-l, Supplementary Fig. 6g-i), but not in the mutant. Ethephon treatment also increased expression levels of the *EIN2L*, *EIL3* and *EIL4* genes in WT plants, but more so for *EIN2L* (Fig. 4l, Supplementary Fig. 6j).

3.5 *EIN2L* gene mediates ABA signaling and promotes stomatal closure

ABA treatment significantly decreased stomatal aperture of WT plants, but had less effect in MU plants (Supplementary Fig. 5a-b). ABA treatment reduced stomatal conductance (41%), net photosynthetic rate (40%), and transpiration rate (35%) in WT plants, while increasing intercellular CO_2 concentration (24%). MU plants showed milder reductions (30%, 31%, 26%) and stable CO_2 levels (Fig. 5a, Supplementary Fig. 5c-e). Additionally, ABA accelerated leaf senescence and reduced chlorophyll content in WT but not MU plants (Supplementary Fig. 5f-g). The insensitivity of MU plants to ABA treatment suggests that *EIN2L* may be involved in mediating ABA signaling and promoting stomatal closure.

Transcription levels of the genes *RBOHD*, *RBOHF*, *NIA1*, and *NIA2* were higher in WT than MU plants independently of ABA treatment (Fig. 5b-e). ABA treatment significantly increased transcription levels of all 4 genes, but more so in WT plants. While ABA treatment significantly increased guard cell NO and ROS levels in WT plants, they were significantly lower in MU plants (Fig. 5f-h). DAB/NBT staining of WT plants showed grater H_2O_2 and O_2^- deposition, and the staining area was significantly larger than that of MU plants (Supplementary Fig. 5h-i). These results suggest that *EIN2L* gene is involved in ABA-induced accumulation of NO and ROS. Similarly, ABA treatment also increased expression levels of the *SLAH1* and *SLAH3* genes to a greater extent in WT plants (Fig. 5i-j). Furthermore, ABA treatment significantly increased expression levels of the *EIN2L*, *EIL3* and *EIL4* genes in WT plants, especially for *EIN2L* (Fig. 5l). Without ABA treatment, *ABF2* and *ABF3* (but not *ABF1*) were more highly expressed in WT plants (Supplementary Fig. 5j-l), while ABA treatment accentuated genotypic differences for all ABF genes. Without ABA treatment, expression levels of the ABA signaling gene *PYL8* and ABA biosynthesis gene *ABA1* didn't vary between genotypes, although the ABA biosynthesis gene *NCED3* was 2.1-fold higher in WT plants than MU plants (Supplementary Fig. 5m-o). Endogenous ABA content of WT plants was 1.85 times higher than MU plants (Supplementary Fig. 5p), consistent with the higher *NCED3* gene expression in WT plants. Meanwhile, ABA treatment significantly increased expression levels of all 3 genes in both genotypes, but more so in WT plants. By affecting expression of ABA signaling and synthesis genes, *EIN2L* was involved in ABA-induced stomatal closure.

Subsequently, we predict potential binding sites of *EIL3* transcription factors to key signaling pathway promoters associated with ethylene/drought / ABA. *EIL3* was predicted to have multiple specific binding sites in the regulatory regions of all target genes, except the promoter region of *ABF1* gene (Supplementary Fig. 7). Thus *EIL3*

may participate in a regulatory network of plant physiological processes by directly regulating the transcription of these genes.

4 DISCUSSION

Ethylene's impacts on stomatal movement, and its interactions with ABA, are often contradictory (Hasan et al., 2024). While ethylene can promote stomatal closure, it can also antagonize ABA-induced stomatal closure thereby attenuating stomatal closure under environmental stresses (Song et al., 2023). Using gene edited (MU) plants with knocked down ethylene signaling (Cheng et al., 2023) demonstrated that *EIN2L*, *EIL3* and *EIL4* are core regulatory elements. The stomata closing signals darkness (Fig. 1e), ethephon (Fig. 4l) and ABA (Fig. 5l) all induced expression of *EIN2L* (especially), *EIL3* and *EIL4*, which rapidly decreased during dark to light transitions (Fig. 1e). Although further studies with single and double knockdown mutants are needed, *EIN2L* seems a critical component of this signaling module since it is specifically expressed in guard cells (Fig. 1f). While ethephon treatment greatly promoted stomatal closure in WT plants, ethylene insensitivity of the mutant attenuated this response (Fig. 4a, Supplementary Fig. 4a-b) and compromised its ABA response (Fig. 5a, Supplementary Fig. 5a-b) thereby diminishing its recovery from drought stress (Fig. 2c-d). Physiological effects of this altered stomatal sensitivity to both ABA and ethylene will depend on how the environment alters dynamics of these hormones *in vivo*.

EIN3 positively mediates ethylene signaling by interacting with EIN2 C-terminal (Binder, 2020; Shao et al., 2024). Since there are as many as 13 EIN3-like elements in soybean genome (Cheng et al., 2023), it is likely that *EIN2L* inhibits downstream ethylene signaling by affecting some of these EIN3 genes in coordination with *EIL3* and *EINL4*. This is consistent with the prediction by PlantPAN 4.0(Chow et al., 2024) of one or more potential *EIN3* binding sites in the promoter region of ethylene/drought/ABA regulatory genes (Supplementary Fig. 7). Although the presence of functionally redundant EIN2s and EIN3s may partially compensate for the absence of EIN2, *EIL3*, and *EIL4*, it seems EIN2, *EIL3*, and *EIL4* collectively mediate stomatal opening (Supplementary Fig. 2a-b). These effects were attributed to altering guard cell ROS and NO levels, since increased expression levels of the ROS synthesizing gene *RBOHD* and the NO synthesizing genes *NIA1* and *NIA2* in the dark (Fig. 3a-d) and following ethephon treatment (Fig. 3b-e, Supplementary Fig. 6a-d) were attenuated in the mutant, accompanied by greater stomatal opening (Fig. 1d, 4a). In addition, ethylene treatment could significantly induce the accumulation of NO and ROS in stomatal guard cells of WT plants, while the levels of NO and ROS in guard cells of MU plants were significantly lower than those of WT plants under the action of ethylene, Fig. 4f-i, Supplementary Fig. 4h-i). Measuring ROS and NO levels is necessary to integrate our gene expression data with models demonstrating that ethylene treatment also upregulates guard cell synthesis of flavonol antioxidants that diminish ROS levels and attenuate ABA-induced stomatal closure (Watkins et al. 2017; Song et al. 2023). Downstream of these signals, the SLOW ANION CHANNELASSOCIATED 1 (SLAC1) gene family plays a key role in regulating stomatal closure, with four

homologues in Arabidopsis having different expression patterns and function (Hedrich & Geiger, 2017). Two soybean homologous genes *SLAH1* and *SLAH3* from the SLAC1 family were selected from the soybean public gene expression database (Almeida-Silva, Pedrosa-Silva, & Venancio, 2023; Oikawa et al., 2018). Their expression increased in darkness (Fig. 3e-f) and following ethephon (Fig. 4j-k, Supplementary Fig. 6e-f) or ABA (Fig. 5j-k) treatment, but less so in the mutant, indicating the EIN2-*EIL3*-*EIL4* regulatory module mediated this process. Thus ethylene signaling seems important in regulating stomatal movement.

Whether light enhances or inhibits ethylene biosynthesis is controversial. Greater ethylene biosynthesis of light-grown Arabidopsis seedlings (Yoon & Kieber, 2013) was associated with light inhibiting hypocotyl elongation by stabilizing the ACS5 protein during the dark-to-light transition (Seo & Yoon, 2019). However, low light (125 µmol m^{-2} s^{-1}) strongly inhibited ethylene production when cut soybean leaf segments were floated on a 1 mM ACC solution in a closed flask or when intact plants were sprayed with ACC, but had no effect on leaf ethylene production of control (unsprayed|) plants in a continuous flow system (Bassi & Spencer, 1983). In contrast, shade treatment (transmitting 25% of outdoor light) promoted foliar expression of ethylene biosynthesis (*SAMS*, *ACS* and *ACO*) and signal transduction (*GmEIN3-1, GmEIN3-2*) genes in soybean (Deng et al., 2024). While darkness promotes expression of the ethylene synthesis genes *ACS* and *ACO* in soybeans (Fig. 3g-j), light inhibits them dependent on the EIN2-*EIL3*-*EIL4* regulatory module. Such feedback regulation of ethylene biosynthesis genes seems important in regulating ethylene production in many species (Rzewuski, G., Sauter, & M., 2008). Although ethylene synthesis peaked during the light period in sorghum (Finlayson, Lee, & Morgan, 1998) and Arabidopsis (Thain et al., 2004) seedlings, additional dark-induced ethylene synthesis may enhance stomatal closure, as stomata of the mutant closed less in the dark (Fig. 1d). Pharmacological approaches may also help unravel ethylene's role in dark-induced stomatal closure. Stomata within epidermal peels of *Commelina benghalensis* remained closed under ethephon treatments in the dark, but opened widely in the presence of the ethylene perception inhibitor $AgNO_3$ (Kar, Parvin, & Laha, 2013). However, different ethylene synthesis and ethylene-mediated physiological responses according to whether excised plant portions or intact plants are measured (as highlighted above) indicate the importance of the gene edited (*EIN2L*, *EIL3* and *EIL4*) mutant plants in determining ethylene's role *in vivo*.

Plants respond to soil drying by reducing stomatal opening to reduce water use, but this limits internal CO_2 concentration, thereby decreasing photosynthesis. The *EIN2L*-*EIL3*-*EIL4* regulatory module could be a switch mediating ABA-ethylene interactions that alter stomatal responses (Fig. 4a, 5a, Supplementary Fig. 4a-b, 5a-b), plant growth and crop yield (Cheng et al., 2023). Soil drying increased root and leaf ABA and ACC (the ethylene precursor) concentrations in soybean (Tamang, Li, Rajasundaram, Lamichhane, & Fukao, 2021), although osmotic stress had variable effects on ethylene signal transduction in soybean roots (X. Wang, Wei, Zhao, Li, & Dong, 2024). While soil drying mediates both ABA-dependent and -independent changes in gene expression (Yoshida, Mogami, & Yamaguchi-Shinozaki, 2014), ABA treatment upregulated *EIN2L*,

EIL3, and *EIL4* gene expression (Fig. 5l) while also promoting the expression of ABA synthesis (*ABA1*, *NCED3* - Supplementary Fig. 4n-o) and receptor (*PYL8* - Supplementary Fig. 5m) genes. The endogenous ABA content of MU plants was consistent with the low level expression of *NCED3*. These changes in ABA biosynthesis and signaling were diminished in the mutant, suggesting the *EIN2L-EIL3-EIL4* regulatory module attenuates a positive feedback cycle regulating ABA homeostasis and responses. Further studies comparing physiological and hormonal responses of the WT and mutant plants to soil drying seem warranted, especially since these genotypes differed in chlorophyll and survival responses. Likely the greater water use of the mutant dried the soil more, compromising survival rates after re-watering (Fig. 2e-f). Although transgenically decreasing ethylene biosynthesis attenuated chlorophyll loss of well-watered and droughted maize plants (Young, Meeley, & Gallie, 2004), greater chlorophyll loss of the *EIN2L*, *EIL3* and *EIL4* gene edited plants (Supplementary Fig. 2a) could be attributed to leaf death following embolism rather than a direct response to attenuated ethylene sensitivity, as ethylene-insensitive plants typically show diminished leaf senescence (Oh et al., 1997).

Overall, the EIN2-*EIL3*-*EIL4* regulatory module plays a key role in regulating typical diurnal responses to light and ABA- and ethylene-mediated stress responses (Fig. 6). While this module regulates ethylene synthesis genes *ACS* and *ACO* during light-dark transitions, and ABA synthesis (*ABA1, NCED3*) and signalling (*PYL8*) genes following ABA treatment, further work is needed to establish how this module regulates hormonal responses to drying soil. Nevertheless, its impacts on physiological and gene expression responses to light and drying soil suggests its agronomic importance. When water resources are abundant, desensitizing stomatal responses (as in the gene edited MU plants) can improve crop productivity but may compromise productivity when water resources are scarce. While developmental adaptations—notably enhanced root system architecture that improves soil water extraction capacity (Dinneny, 2019; Gupta, Rico-Medina, & Caño-Delgado, 2020)—actively sustain hydro-homeostasis and promote drought tolerance (Fig. 6). These findings collectively illustrate the complexity of plant drought resistance mechanisms, which operate through both stomatal-dependent regulation (e.g., transpiration control) and stomatal-independent strategies (e.g., hydraulic architecture optimization). This multilevel coordination suggests that crop improvement programs should adopt integrated approaches targeting complementary drought adaptation pathways.

ACKNOWLEDGMENTS

We would like to thank Academician Yaoguang Liu of South China Agricultural University for providing the CRISPR-Cas9 vectors.

Funding

This work was financially supported by the National Natural Science Foundation of China (No. 32172079) and Outstanding Talents Team Project of Department of Science and Technology of Jilin Province (No. 20240601063RC).

CONFLICT OF INTEREST STATEMENT

The authors declare no conflict of interest.

REFERENCES

Almeida-Silva, F., Pedrosa-Silva, F., & Venancio, T. M. (2023). The Soybean Expression Atlas v2: A comprehensive database of over 5000 RNA-seq samples. *The Plant Journal, 116,* 1041-1051.

Alonso, J. M., Stepanova, A. N., Solano, R., Wisman, E., Ferrari, S., Ausubel, F. M., & Ecker, J. R. (2003). Five components of the ethylene-response pathway identified in a screen for weak ethylene-insensitive mutants in Arabidopsis. *Proceedings of the National Academy of Sciences of the United States of America, 100,* 2992-2997.

An, F., Zhao, Q., Ji, Y., Li, W., Jiang, Z., Yu, X., Guo, H. (2010). Ethylene-induced stabilization of ETHYLENE INSENSITIVE3 and EIN3-LIKE1 is mediated by proteasomal degradation of EIN3 binding F-box 1 and 2 that requires EIN2 in Arabidopsis. *The Plant Cell, 22,* 2384-2401.

Anfang, M., & Shani, E. (2021). Transport mechanisms of plant hormones. *Current Opinion in Plant Biology, 63,* 102055.

Azoulay-Shemer, T., Schulze, S., Nissan-Roda, D., Bosmans, K., Shapira, O., Weckwerth, P., Schroeder, J. I. (2023). A role for ethylene signaling and biosynthesis in regulating and accelerating CO_2 - and abscisic acid-mediated stomatal movements in Arabidopsis. *New Phytologist, 238,* 2460-2475.

Bassi, P. K., & Spencer, M. S. (1983). Does light inhibit ethylene production in leaves? *Plant Physiology, 73,* 758-760.

Binder, B. M. (2020). Ethylene signaling in plants. *Journal of Biological Chemistry, 295,* 7710-7725.

Ceusters, J., & Van de Poel, B. (2018). Ethylene Exerts Species-Specific and Age-Dependent Control of Photosynthesis. *Plant Physiology, 176,* 2601-2612.

Chang, C., Kwok, S. F., Bleecker, A. B., & Meyerowitz, E. M. (1993). Arabidopsis ethylene-response gene ETR1: similarity of product to two-component regulators. *Science, 262,* 539-544.

Chao, Q., Rothenberg, M., Solano, R., Roman, G., Terzaghi, W., & Ecker, J. R. (1997). Activation of the ethylene gas response pathway in Arabidopsis by the nuclear protein ETHYLENE-INSENSITIVE3 and related proteins. *Cell, 89,* 1133-1144.

Chen, C., Chen, H., Zhang, Y., Thomas, H. R., Frank, M. H., He, Y., & Xia, R. (2020). TBtools: An Integrative Toolkit Developed for Interactive Analyses of Big Biological Data. *Molecular Plant*, 13(8), 1194-1202.

Chen, C., Wu, Y., Li, J., Wang, X., Zeng, Z., Xu, J., Xia, R. (2023). TBtools-II: A "one for all, all for one" bioinformatics platform for biological big-data mining. *Molecular Plant*, 16(11), 1733-1742.

Chen, L., Dodd, I. C., Davies, W. J., & Wilkinson, S. (2013). Ethylene limits abscisic acid- or soil drying-induced stomatal closure in aged wheat leaves. *Plant, Cell & Environment, 36,* 1850-1859.

Cheng, Y., Li, Y., Yang, J., He, H., Zhang, X., Liu, J., & Yang, X. (2023). Multiplex CRISPR-Cas9 knockout of *EIL3*, *EIL4*, and *EIN2L* advances soybean flowering time and pod set. *BMC Plant Biology, 23,* 519.

Chow, C. N., Yang, C. W., Wu, N. Y., Wang, H. T., Tseng, K. C., Chiu, Y. H., Chang, W. C. (2024). PlantPAN 4.0: updated database for identifying conserved non-coding sequences and exploring dynamic transcriptional regulation in plant promoters. *Nucleic Acids Research*, 52(D1), D1569-D1578.

Cui, MY, Lin, YC, YG, Efferth, ZH. (2015). Ethylene increases accumulation of compatible solutes and decreases oxidative stress to improve plant tolerance to water stress in Arabidopsis. *Journal of Integrative Plant Biology, 58, 1*93-201.

Deng, J., Huang, X., Chen, J., Vanholme, B., Guo, J., He, Y., Liu, J. (2024). Shade stress triggers ethylene biosynthesis to accelerate soybean senescence and impede nitrogen remobilization. *Plant Physiology and Biochemistry, 210,* 108658.

Desikan, R., Last, K., Harrett-Williams, R., Tagliavia, C., Harter, K., Hooley, R., Neill, S. J. (2006). Ethylene-induced stomatal closure in Arabidopsis occurs via At*rbohF*-mediated hydrogen peroxide synthesis. *The Plant Journal, 47*, 907-916.

Fatma, M., Asgher, M., Iqbal, N., Rasheed, F., Sehar, Z., Sofo, A., & Khan, N. A. (2022). Ethylene Signaling under Stressful Environments: Analyzing Collaborative Knowledge. *Plants -Basel, 11,* 2211.

Finlayson, S. A., Lee, I. J., & Morgan, P. W. (1998). Phytochrome B and the Regulation of Circadian Ethylene Production in Sorghum. *Plant Physiology, 116,* 17-25.

Gao, L., Lv, Q., Wang, L., Han, S., Wang, J., Chen, Y., . . . He, Y. (2024). Abscisic acid-mediated autoregulation of the MYB41-BRAHMA module enhances drought tolerance in Arabidopsis. *Plant Physiology, 196*, 1608-1626.

Gayatri, G., Agurla, S., & Raghavendra, A. S. (2013). Nitric oxide in guard cells as an important secondary messenger during stomatal closure. *Frontiers In Plant Science, 4*, 425.

Ge, X. M., Cai, H. L., Lei, X., Zhou, X., Yue, M., & He, J. M. (2015). Heterotrimeric G protein mediates ethylene-induced stomatal closure via hydrogen peroxide synthesis in Arabidopsis. *The Plant Journal, 82*, 138-150.

Gong, L., Liu, X. D., Zeng, Y. Y., Tian, X. Q., Li, Y. L., Turner, N. C., & Fang, X. W. (2021). Stomatal morphology and physiology explain varied sensitivity to abscisic acid across vascular plant lineages. *Plant Physiology, 186*, 782-797.

Gunderson, C. A., & Taylor, G. E. (1991). Ethylene Directly Inhibits Foliar Gas Exchange in Glycine max. *Plant Physiology, 95*, 337-339.

Gupta, A., Rico-Medina, A., & Caño-Delgado, A. I. (2020). The physiology of plant responses to drought. *Science, 368*, 266-269.

Hao, F., Zhao, S., Dong, H., Zhang, H., Sun, L., & Miao, C. (2010). *Nia1* and *Nia2* are involved in exogenous salicylic acid-induced nitric oxide generation and stomatal closure in Arabidopsis. *Journal of Integrative Plant Biology, 52*, 298-307.

Hasan, M. M., Liu, X. D., Yao, G. Q., Liu, J., & Fang, X. W. (2024). Ethylene-mediated stomatal responses to dehydration and rehydration in seed plants. *Journal of Experimental Botany, 176*.

Hedrich, R., & Geiger, D. (2017). Biology of SLAC1-type anion channels - from nutrient uptake to stomatal closure. *New Phytologist, 216*, 46-61.

Hua, J., Chang, C., Sun, Q., & Meyerowitz, E. M. (1995). Ethylene insensitivity conferred by Arabidopsis ERS gene. *Science, 269*, 1712-1714.

Iglesias-Moya, J., Abreu, A. C., Alonso, S., Torres-García, M. T., Martínez, C., Fernández, I., & Jamilena, M. (2023). Physiological and metabolomic responses of the ethylene insensitive squash mutant etr2b to drought. *Plant Science, 336*, 111853.

Kar, R. K., Parvin, N., & Laha, D. (2013). Differential role of ethylene and hydrogen peroxide in dark-induced stomatal closure. *Pakistan Journal of Biological Sciences, 16*, 1991-1996.

Kawakami, E. M., Oosterhuis, D. M., & Snider, J. L. (2010). Physiological Effects of 1-Methylcyclopropene on Well-Watered and Water-Stressed Cotton Plants. *Journal of Plant Growth Regulation, 29*, 280-288.

Khan, N. A., Ferrante, A., Khan, M. I. R., & Poor, P. (2023). Editorial: Ethylene: a key regulatory molecule in plants, Volume II. *Frontiers in Plant Science, 14*, 1222462.

Kim, T. H., Böhmer, M., Hu, H., Nishimura, N., & Schroeder, J. I. (2010). Guard cell signal transduction network: advances in understanding abscisic acid, CO2, and Ca2+ signaling. *Annual Review of Plant Biology*, 61, 561-591.

Kuromori, T., Seo, M., & Shinozaki, K. (2018). ABA Transport and Plant Water Stress Responses. Trends *Plant Science*, 23(6), 513-522.

Liu, X. D., Zeng, Y. Y., Zhang, X. Y., Tian, X. Q., Hasan, M. M., Yao, G. Q., & Fang, X. W. (2023). Polyamines inhibit abscisic acid-induced stomatal closure by scavenging hydrogen peroxide. *Physiologia Plantarum, 175*, e13903.

Majeed, S., Nawaz, F., Naeem, M., Ashraf, M. Y., Ejaz, S., Ahmad, K. S., . . . Mehmood, K. (2020). Nitric oxide regulates water status and associated enzymatic pathways to inhibit nutrients imbalance in maize (*Zea mays L.*) under drought stress. Plant Physiology and Biochemistry*, 155*, 147-160.

Oh, S. A., Park, J. H., Lee, G. I., Paek, K. H., Park, S. K., & Nam, H. G. (1997). Identification of three genetic loci controlling leaf senescence in *Arabidopsis thaliana*. *The Plant Journal, 12*, 527-535.

Oikawa, T., Ishimaru, Y., Munemasa, S., Takeuchi, Y., Washiyama, K., Hamamoto, S., Ueda, M. (2018). Ion Channels Regulate Nyctinastic Leaf Opening in *Samanea saman*. *Current Biology, 28*, 2230-2238, e2237.

Pallaghy, C. K., & Raschke, K. (1972). No stomatal response to ethylene. *Plant Physiology, 49*, 275-276.

Perez-Perez, J. G., Puertolas, J., Albacete, A., & Dodd, I. C. (2020). Alternation of wet and dry sides during partial rootzone drying irrigation enhances leaf ethylene evolution. *Environmental and Experimental Botany, 176*, 104095.

Potuschak, T., Lechner, E., Parmentier, Y., Yanagisawa, S., Grava, S., Koncz, C., & Genschik, P. (2003). EIN3-dependent regulation of plant ethylene hormone signaling by two arabidopsis F box proteins: EBF1 and EBF2. *Cell, 115*, 679-689.

Rzewuski, G., Sauter, & M. (2008). Ethylene biosynthesis and signaling in rice. *Plant Science, 175*, 32-42.

Schmittgen, T. D., & Livak, K. J. (2008). Analyzing real-time PCR data by the comparative C(T) method. *Nature Protocols, 3*, 1101-1108.

Schroeder, J. I., & Keller, B. U. (1992). Two types of anion channel currents in guard cells with distinct voltage regulation. *Proceedings of the National Academy of Sciences of the United States of America, 89*, 5025-5029.

Seo, D. H., & Yoon, G. M. (2019). Light-induced stabilization of ACS contributes to hypocotyl elongation during the dark-to-light transition in Arabidopsis seedlings. *The Plant Journal, 98*, 898-911.

Shen, C., Zhang, Y., Li, Q., Liu, S., He, F., An, Y., Xia, X. (2021). PdGNC confers drought tolerance by mediating stomatal closure resulting from NO and H_2O_2 production via the direct regulation of PdHXK1 expression in Populus. *New Phytologist, 230*, 1868-1882.

Shao, Z., Bian, L., Ahmadi, S. K., Daniel, T. J., Belmonte, M. A., Burns, J. G., Qiao, H. (2024). Nuclear pyruvate dehydrogenase complex regulates histone acetylation and transcriptional regulation in the ethylene response. *Science Advances*, 10(30), eado2825.

Shi, C., Chen, F., Peng, T., & She, X. (2017). Role of Cytoplasmic Alkalization and Nitric Oxide in Ethylene-induced Stomatal Closure in Arabidopsis. *International Journal of Agriculture and Biology, 19*, 1220-1226.

Solano, R., Stepanova, A., Chao, Q., & Ecker, J. R. (1998). Nuclear events in ethylene signaling: a transcriptional cascade mediated by ETHYLENE-INSENSITIVE3 and ETHYLENE-RESPONSE-FACTOR1. *Genes & Development, 12*, 3703-3714.

Song, Z., Zhao, L., Ma, W., Peng, Z., Shi, J., Pan, F., Wang, B. (2023). Ethylene inhibits ABA-induced stomatal closure via regulating NtMYB184-mediated flavonol biosynthesis in tobacco. *Journal of Experimental Botany, 74*, 6735-6748.

Tamang, B. G., Li, S., Rajasundaram, D., Lamichhane, S., & Fukao, T. (2021). Overlapping and stress-specific transcriptomic and hormonal responses to flooding and drought in soybean. *The Plant Journal, 107*, 100-117.

Tanaka, Y., Sano, T., Tamaoki, M., Nakajima, N., Kondo, N., & Hasezawa, S. (2005). Ethylene inhibits abscisic acid-induced stomatal closure in Arabidopsis. *Plant Physiology, 138*, 2337-2343.

Tanaka, Y., Sano, T., Tamaoki, M., Nakajima, N., Kondo, N., & Hasezawa, S. (2006). Cytokinin and auxin inhibit abscisic acid-induced stomatal closure by enhancing ethylene production in Arabidopsis. *Journal of Experimental Botany, 57*, 2259-2266.

Taylor, G. E., & Gunderson, C. A. (1986). The response of foliar gas exchange to exogenously applied ethylene. *Plant Physiology, 82*, 653-657.

Thain, S. C., Vandenbussche, F., Laarhoven, L. J., Dowson-Day, M. J., Wang, Z. Y., Tobin, E. M., . . . Van Der Straeten, D. (2004). Circadian rhythms of ethylene emission in Arabidopsis. *Plant Physiology, 136*, 3751-3761.

Vine, J. H., Noiton, D., Plummer, J. A., Baleriola-Lucas, C., & Mullins, M. G. (1987). Simultaneous quantitation of indole 3-acetic Acid and abscisic Acid in small samples of plant tissue by gas chromatography/mass spectrometry/selected ion monitoring. *Plant Physiology*, 85(2), 419-422.

Wang, W., Esch, J. J., Shiu, S. H., Agula, H., Binder, B. M., Chang, C., Bleecker, A. B. (2006). Identification of important regions for ethylene binding and signaling in the transmembrane domain of the ETR1 ethylene receptor of Arabidopsis. *The Plant Cell, 18*, 3429-3442.

Wang, X., Wei, X., Zhao, W., Li, X., & Dong, S. (2024). Elucidating hormone transduction and the protein response of soybean roots to drought stress based on ultra performance liquid chromatography–tandem mass spectrometry and four-dimensional data-independent acquisition. *Environmental and Experimental Botany, 224,* 105820.

Wang, Y., Liu, C., Li, K., Sun, F., Hu, H., Li, X., Li, X. (2007). Arabidopsis EIN2 modulates stress response through abscisic acid response pathway. *Plant Molecular Biology, 64*, 633-644.

Watkins, J. M., Hechler, P. J., & Muday, G. K. (2014). Ethylene-induced flavonol accumulation in guard cells suppresses reactive oxygen species and moderates stomatal aperture. *Plant Physiology, 164*, 1707-1717.

Wei, H., Cheng, Y., Sun, Y., Zhang, X., He, H., & Liu, J. (2021). Genome-Wide Identification of the ARF Gene Family and ARF3 Target Genes Regulating Ovary Initiation in Hazel via ChIP Sequencing. *Frontiers In Plant Science, 12*, 715820.

Xin, L. J. L. G. H. L. L. (2010). Ethylene-induced nitric oxide production and stomatal closure in *Arabidopsis thaliana* depending on changes in cytosolic pH. *Science Bulletin, 55*, 2403-2409.

Xu, C., Shan, J., Liu, T., Wang, Q., Ji, Y., Zhang, Y., Zhao, L. (2023). CONSTANS-LIKE 1a positively regulates salt and drought tolerance in soybean. *Plant Physiology*, 191(4), 2427-2446.

Yoon, G. M., & Kieber, J. J. (2013). 14-3-3 regulates 1-aminocyclopropane-1-carboxylate synthase protein turnover in Arabidopsis. *The Plant Cell, 25*, 1016-1028.

Yoshida, T., Mogami, J., & Yamaguchi-Shinozaki, K. (2014). ABA-dependent and ABA-independent signaling in response to osmotic stress in plants. *Current Opinion in Plant Biology, 21*, 133-139.

Young, T. E., Meeley, R. B., & Gallie, D. R. (2004). ACC synthase expression regulates leaf performance and drought tolerance in maize. *The Plant Journal, 40*, 813-825.

Zhang, F., Wang, L., Qi, B., Zhao, B., Ko, E. E., Riggan, N. D., Qiao, H. (2017). EIN2 mediates direct regulation of histone acetylation in the ethylene response. *Proceedings of the National Academy of Sciences of the United States of America, 114*, 10274-10279.

Zhang, L., Huang, J., Su, S., Wei, X., Yang, L., Zhao, H., Duan, Q. (2021). FERONIA receptor kinase-regulated reactive oxygen species mediate self-incompatibility in Brassica rapa. *Current Biology*, 31(14), 3004-3016.e3004.

Zhang, T. Y., Li, Z. Q., Zhao, Y. D., Shen, W. J., Chen, M. S., Gao, H. Q., He, J. M. (2021). Ethylene-induced stomatal closure is mediated via MKK1/3-MPK3/6 cascade to EIN2 and EIN3. *Journal of Integrative Plant Biology, 63*, 1324-1340.

FIGURE LEGENDS

Figure 1. *EIN2L* plays an important role in regulating stomatal movement. **a)** Nocturnal leaf movement (images taken above the plants) of WT and MU plants after 0.5 h (ZT2.5) and 0.75 h (ZT2.75) of dark and 0.75 h (ZT3.5) of light treatments. ZT, zeitgeber time. Photoperiod was set from 08:00h (ZT0) to 20:00 h (ZT12). The white and black bars represent light and dark states, respectively. Scale, 5 cm. **b)** Normalized leaf area (calculated using the software ImageJ from images taken above the plants) of WT and MU plants under light (white bars) and dark (black bars) changes. Symbols are means ± SD (n =3, ****p < 0.0001; T-test). **c)** Stomatal density of WT and MU plants (ns, p > 0.05; T-test). **d)** Stomatal conductance of WT and MU plants under light (white bars) and dark (black bars) changes respectively. Symbols are mean ± SD (n =9，**p<0.01; ****p < 0.0001; T-test). **e)** Expression of *EIN2L*, *EIL3* and *EIL4* genes under light and dark conditions in WT plants. Data are means ± SD (n =9, derived from three biological replicates and three technical replicates, ****p < 0.0001; T-test). **f)** Representative images of guard cells after immunohistochemical analysis captured using 20× magnification. Scale, 10 μm.

Figure 2. Impaired stomatal closure reduced drought resistance of the mutant. **a)** Isolated leaf image and **b)** Isolated leaf water loss rate survival rate. Data expressed as means ±SD (n =9，from 3 independent experiments). **c)** Plant images, **d)** Root images, **e)** Shoot relative growth rate, **f)** Survival rates, **g)** Plant water content, **h)** Soil water content, **i)** Stomatal conductance, **j)** Total number of roots and **k)** Total root length of soil-grown plants at day 7 (after drought stress) and day 14 (after rehydration). Scale, 5 cm. Data are means ± SD (n=36, from 3 independent experiments). Asterisks indicate significant differences (ns, p> 0.05, *p<0.05, **p<0.01, ****p < 0.0001; T-test). Different letters on the top of the bars indicate significant differences at p < 0.05 level.

Figure 3. The expression level of NO and ROS synthesis related genes, anion channel SLAHs and ethylene biosynthesis genes during light-darkness transition. The expression level of **a)** *RBOHF*, **b)** *RBOHD*, **c)** *NIA1*, **d)** *NIA2*, **e)** *SLAH1*, **f)** *SLAH3* **g)** *ACS1*, **h)** *ACS6*, **i)** *ACO1* and **j)** *ACO4* genes of MU and WT plants under light and dark treatment. Values are the mean ± SD (n =9, derived from three biological replicates and three technical replicates). Different letters on the top of the bars indicate significant differences at p < 0.05 level, and two-way ANOVA for treatment (T) and genotype (G) is shown in each panel. ***p < 0.001.

Figure 4. *EIN2L* gene mediates ethylene signaling related to NO and ROS, promoting stomatal closure. **a)** Stomatal conductance of WT and MU plants under ETH treatment. Bars are means ± SD (n =9). The expression level of **b)** *RBOHF*, **c)** *RBOHD*, **d)** *NIA1* and **e)** *NIA2* genes of MU and WT plants under ETH treatment. (Values are means ± SD, n=9, derived from three biological replicates and three technical replicates). **f–i)** NO and ROS fluorescence images (Scale: 10 μm) and fluorescence intensity in guard

cells (mean ± SD, n = 5). The expression level of **j)** *SLAH1* and **k)** *SLAH3* genes of MU and WT plants under ETH treatment (Values are means ± SD, n=9). The expression level of gene *EIN2L*, *EIL3* and *EIL4* under ETH treatment (Values are means ± SD, n=9). Different letters on the top of the bars indicate significant differences at $p < 0.05$ level, and two-way ANOVA for treatment (T) and genotype (G) is shown in panel. ***$p < 0.001$.

Figure 5. *EIN2L* gene mediates ABA signaling related to NO and ROS and promotes stomatal closure. **a)** Stomatal conductance of WT and MU plants under ABA treatment. Bars are means ± SD (n =9). The expression level of **b)** *RBOHF*, **c)** *RBOHD*, **d)** *NIA1* and **e)** *NIA2* genes of MU and WT plants under ABA treatment. (Values are means ± SD, n =9, derived from three biological replicates and three technical replicates). **f–i)** NO and ROS fluorescence images (Scale: 10 μm) and fluorescence intensity in guard cells (mean ± SD, n=5). The expression level of **j)** *SLAH1* and **k)** *SLAH3* genes of MU and WT plants under ABA treatment (Values are the mean ± SD, n =9). The expression level of gene *EIN2L*, *EIL3* and *EIL4* under ABA treatment (Values are means ± SD, n=9). Different letters on the top of the bars indicate significant differences at $p < 0.05$ level, and two-way ANOVA for treatment (T) and genotype (G) is shown in panel. ***$p < 0.001$.

Figure 6. A potential model of *EIN2L*, *EIL3*, and *EIL4* in promoting drought-induced ABA and light-darkness transition response. When water is not sufficient, drought-induced ABA synthesis through *NCED3* and *ABA1* occurs, which then promotes *EIN2L*, *EIL3*, and *EIL4* expression through ABA receptors PYLs and ABA signaling pathway. *EIN2L*, *EIL3*, and *EIL4*-induced stomatal closure increases through the synthesis of ROS by NADPH oxidase-dependent pathways and NO by Nitrate reductase-dependent pathways synergistically with the activation of SLAHs. *EIN2L*, *EIL3*, and *EIL4* also mediates the dark-induced ethylene facilitated stomatal closure process. *EIN2L*, *EIL3*, and *EIL4* have positive feedback effect on ABA synthesis and ethylene synthesis by regulating the rate limiting enzymes *NCED3* and *ABA1* of ABA and the rate limiting enzymes *ACS1/6* and *ACO1/4* of ethylene synthesis. *EIN2L*, *EIL3*, and *EIL4* forms a regulating module, controlling water loss and CO_2 entrance by regulating stomatal movement, which balance the photosynthetic efficiency and drought tolerance, the red downward arrow indicates reduce.

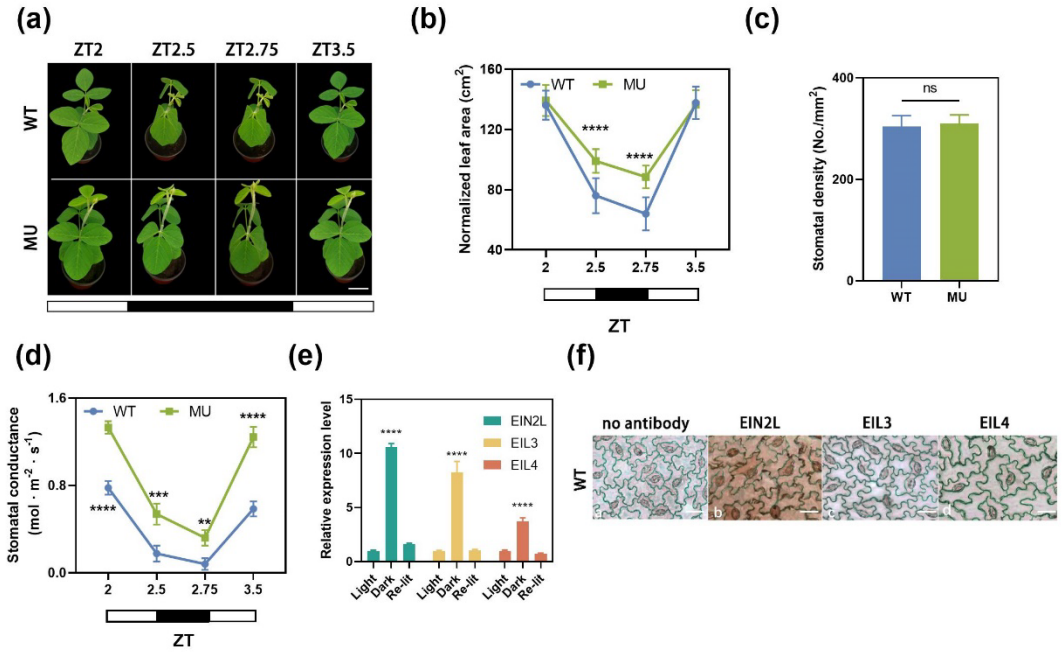

Figure 1. *EIN2L* plays an important role in regulating stomatal movement. **a)** Nocturnal leaf movement (images taken above the plants) of WT and MU plants after 0.5 h (ZT2.5) and 0.75 h (ZT2.75) of dark and 0.75 h (ZT3.5) of light treatments. ZT, zeitgeber time. Photoperiod was set from 08:00h (ZT0) to 20:00 h (ZT12). The white and black bars represent light and dark states, respectively. Scale, 5 cm. **b)** Normalized leaf area (calculated using the software ImageJ from images taken above the plants) of WT and MU plants under light (white bars) and dark (black bars) changes. Symbols are means ± SD (n =3, ****p < 0.0001; T-test). **c)** Stomatal density of WT and MU plants (ns, p > 0.05; T-test). **d)** Stomatal conductance of WT and MU plants under light (white bars) and dark (black bars) changes respectively. Symbols are mean ± SD (n =9，**p<0.01; ****p < 0.0001; T-test). **e)** Expression of *EIN2L*, *EIL3* and *EIL4* genes under light and dark conditions in WT plants. Data are mean ± SD (n =9, derived from three biological replicates and three technical replicates, ****p < 0.0001; T-test). **f)** Representative images of guard cells after immunohistochemical analysis captured using 20× magnification. Scale, 10 μm.

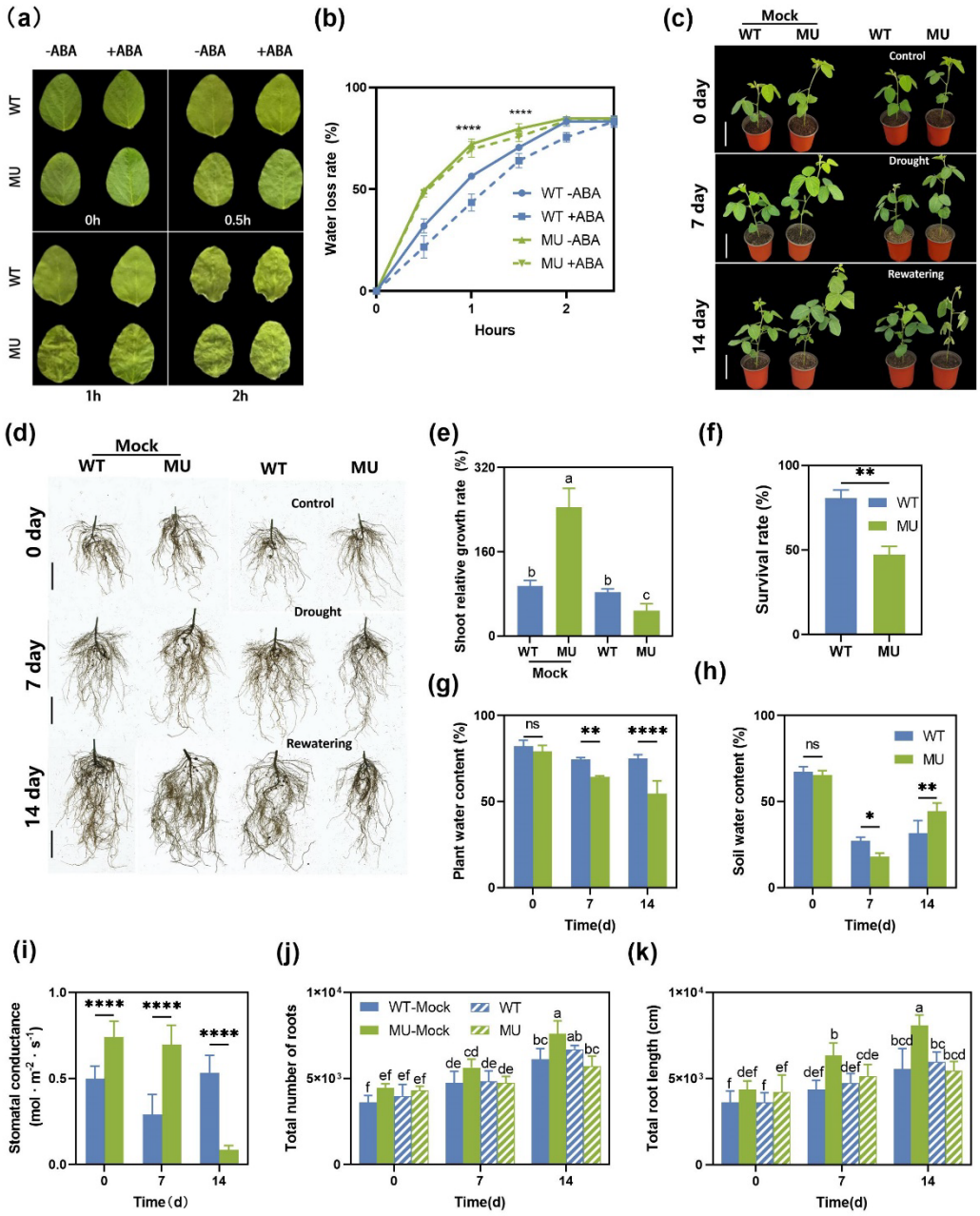

888

889 **Figure 2.** Impaired stomatal closure reduced drought resistance of the mutant. **a)** Isolated leaf image
890 and **b)** Isolated leaf water loss rate survival rate. Data expressed as means ±SD (n =9， from 3
891 independent experiments). **c)** Plant images, **d)** Root images, **e)** Shoot relative growth rate, **f)**
892 Survival rates, **g)** Plant water content, **h)** Soil water content, **i)** Stomatal conductance, **j)** Total
893 number of roots and **k)** Total root length of soil-grown plants at day 7 (after drought stress) and day
894 14 (after rehydration). Scale, 5 cm. Data are means ± SD (n=36, from 3 independent experiments).
895 Asterisks indicate significant differences (ns, p> 0.05, *p<0.05, **p<0.01, ****p < 0.0001; T-test).
896 Different letters on the top of the bars indicate significant differences at p < 0.05 level.

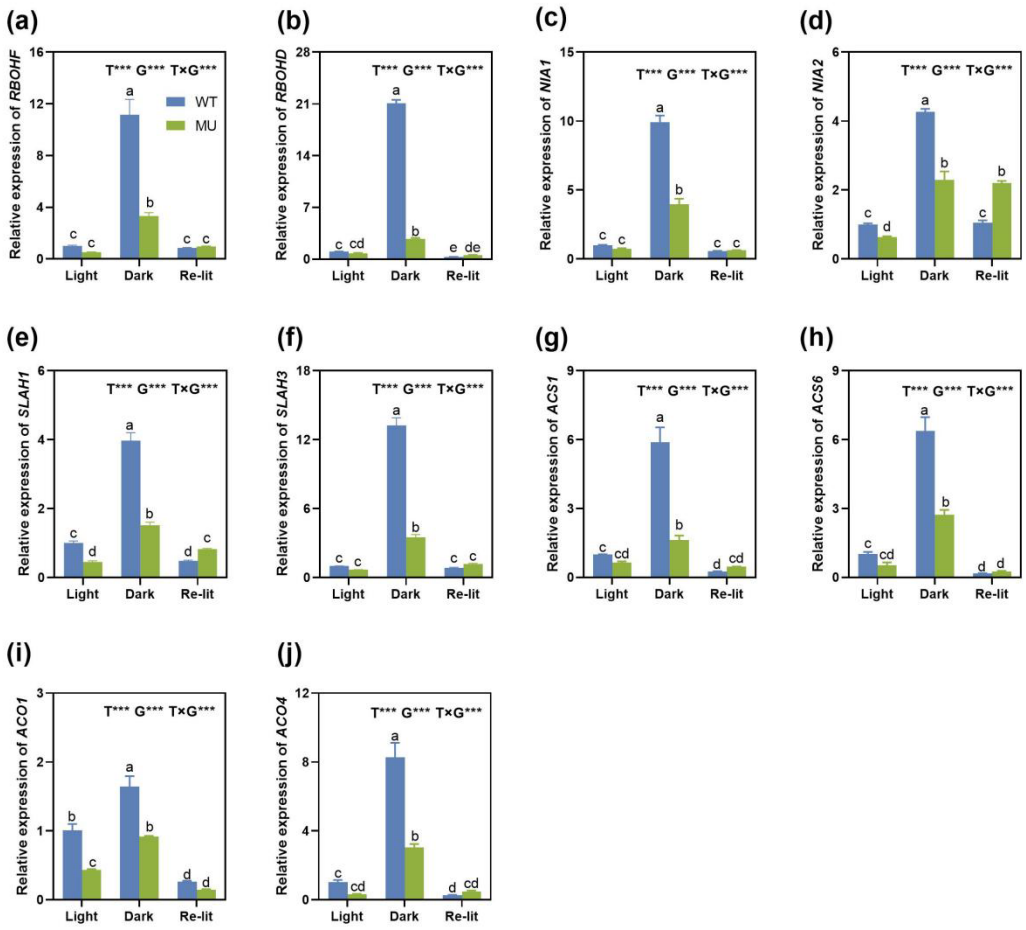

Figure 3. The expression level of NO and ROS synthesis related genes, anion channel SLAHs and ethylene biosynthesis genes during light-darkness transition. The expression level of **a)** *RBOHF*, **b)** *RBOHD*, **c)** *NIA1*, **d)** *NIA2*, **e)** *SLAH1*, **f)** *SLAH3*, **g)** *ACS1*, **h)** *ACS6*, **i)** *ACO1* and **j)** *ACO4* genes of MU and WT plants under light and dark treatment. Values are the mean ± SD (n =9, derived from three biological replicates and three technical replicates). Different letters on the top of the bars indicate significant differences at $p < 0.05$ level, and two-way ANOVA for treatment (T) and genotype (G) is shown in each panel. ***$p < 0.001$

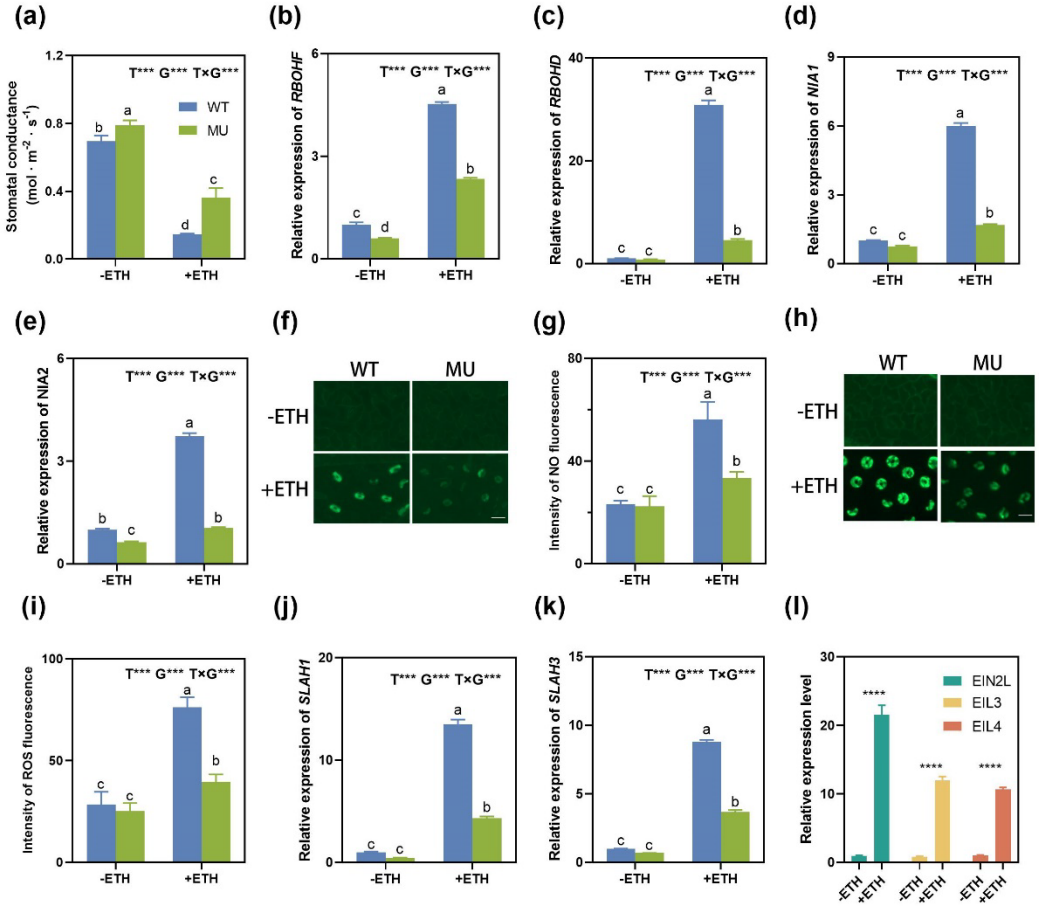

Figure 4. EIN2L gene mediates ethylene signaling related to NO and ROS, promoting stomatal closure. **a)** Stomatal conductance of WT and MU plants under ETH treatment. Bars are means ± SD (n =9). The expression level of **b)** *RBOHF*, **c)** *RBOHD*, **d)** *NIA1* and **e)** *NIA2* genes of MU and WT plants under ETH treatment. (Values are means ± SD, n=9, derived from three biological replicates and three technical replicates). f–i) NO and ROS fluorescence images (Scale: 10 μm) and fluorescence intensity in guard cells (mean ± SD, n = 5). The expression level of **j)** *SLAH1* and **k)** *SLAH3* genes of MU and WT plants under ETH treatment (Values are means ± SD, n=9). **l)** The expression level of gene *EIN2L*, *EIL3* and *EIL4* under ETH treatment (Values are means ± SD, n=9). Different letters on the top of the bars indicate significant differences at $p < 0.05$ level, and two-way ANOVA for treatment (T) and genotype (G) is shown in panel. ***$p < 0.001$.

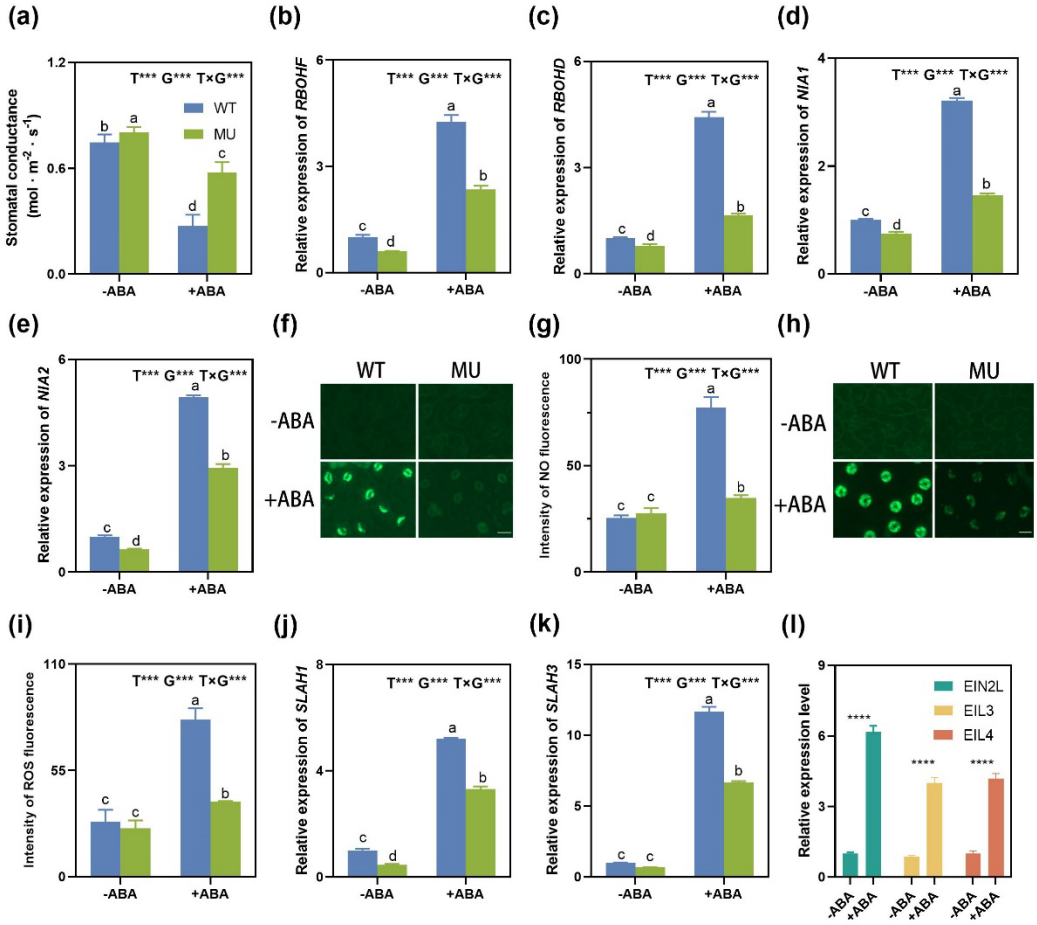

Figure 5. EIN2L gene mediates ABA signaling related to NO and ROS and promotes stomatal closure. **a)** Stomatal conductance of WT and MU plants under ABA treatment. Bars are means ± SD (n =9). The expression level of **b)** *RBOHF*, **c)** *RBOHD*, **d)** *NIA1* and **e)** *NIA2* genes of MU and WT plants under ABA treatment. (Values are means ± SD, n =9, derived from three biological replicates and three technical replicates). **f–i)** NO and ROS fluorescence images (Scale: 10 μm) and fluorescence intensity in guard cells (mean ± SD, n=5). The expression level of **j)** *SLAH1* and **k)** *SLAH3* genes of MU and WT plants under ABA treatment (Values are the mean ± SD, n =9). **l)** The expression level of gene *EIN2L*, *EIL3* and *EIL4* under ABA treatment (Values are means ± SD, n=9). Different letters on the top of the bars indicate significant differences at $p < 0.05$ level, and two-way ANOVA for treatment (T) and genotype (G) is shown in panel. ***$p < 0.001$.

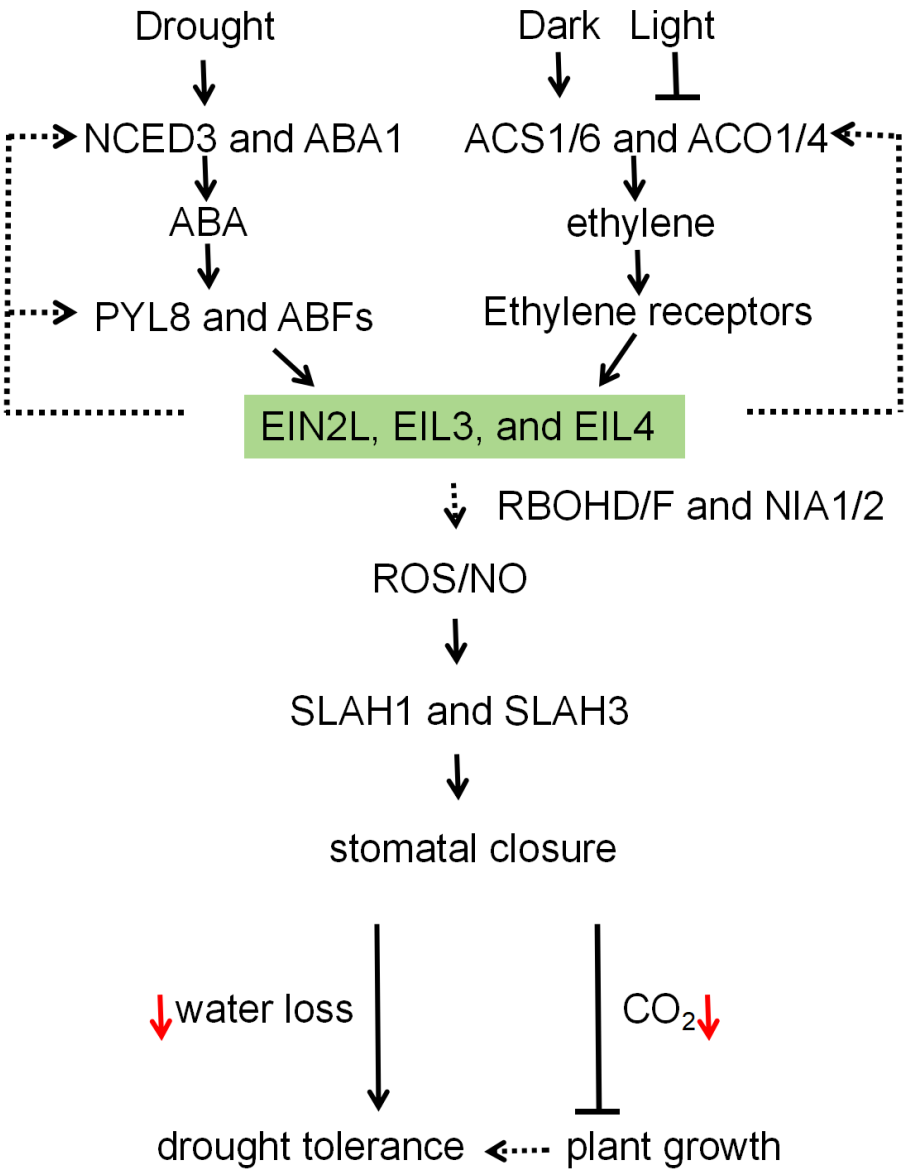

Figure 6. A potential model of *EIN2L*, *EIL3*, and *EIL4* in promoting drought-induced ABA and light-darkness transition response. When water is not sufficient, drought-induced ABA synthesis through *NCED3* and *ABA1* occurs, which then promotes *EIN2L*, *EIL3*, and *EIL4* expression through ABA receptors PYLs and ABA signaling pathway. *EIN2L*, *EIL3*, and *EIL4*-induced stomatal closure increases through the synthesis of ROS by NADPH oxidase-dependent pathways and NO by Nitrate reductase-dependent pathways synergistically with the activation of SLAHs. *EIN2L*, *EIL3*, and *EIL4* also mediates the dark-induced ethylene facilitated stomatal closure process. *EIN2L*, *EIL3*, and *EIL4* have positive feedback effect on ABA synthesis and ethylene synthesis by regulating the rate limiting enzymes *NCED3* and *ABA1* of ABA and the rate limiting enzymes *ACS1/6* and *ACO1/4* of ethylene synthesis. *EIN2L*, *EIL3*, and *EIL4* forms a regulating module, controlling water loss and CO_2 entrance by regulating stomatal movement, which balance the photosynthetic efficiency and drought tolerance, the red downward arrow indicates reduce.